# Oceanic Turbulence in a Zonostrophic regime, numerical results

Alexandre MASSON, Lennard MILLER

June 18, 2024

## 1 Introduction

One of the special features of turbulent flow on a rotating sphere is its potential to evolve into a Zonostrophic regime. This is characterized by relatively large-scale, primarily zonal flow, sometimes forming belt-like shapes around planets. The ocean is a very turbulent place ($Re \sim 10^{10}$) interacting with boundaries (continents), which can disrupt the belt pattern we observe when no physical boundaries are present. It is then interesting to compare two cases, a periodic with a bounded one.

This report presents results of an idealized simulation of turbulent flows on a rotating planet with different boundary conditions (periodic closed). After introducing the parameters controlling the different regimes, we will present the results for a periodic domain, followed by those for a closed domain.

## 2 Governing Parameter

### 2.1 Model Details

The numerical simulation is based on a quasi-geostrophic model with one layer. The energy is injected through stochastic forcing at a certain input wavenumber $k_f$.

The vorticity equation is written :

$$\frac{\partial \nabla^2 \psi}{\partial t} + J(\psi, \nabla^2 \psi) + \beta \frac{\partial \psi}{\partial x} = \epsilon F - r\nabla^2 \psi - \nu \nabla^n (\Delta \psi) \tag{1}$$

The physical parameters appearing in the problem are:

- $\beta$: is the Rossby parameter
- $\epsilon$: the energy input $m^2/s^3$
- $r$: the linear drag
- $\nu$: the kinematic hyper viscosity
- $n$: the integer controlling hyper viscosity "efficiency" (see the part 2.2)

The resolution can also be changed, depending on the viscosity dissipation scale as explained in the following section.

### 2.2 Energy dissipation scales

It's useful to know at which scale the energy get dissipated so we can adjust the parameters to reach the energy balance in a reasonable time for the simulations.
The time scale for drag to remove energy is approximately: $t \sim \frac{1}{r}$
The non-linear time scale writes : $t_{nl} \sim \frac{1}{Uk}$ It is also called the eddy turnover turbulent time scale.
We balance the non-linear term and the drag to find a characteristic scale where turbulence is removed by drag.

When reaching the energy balance, U is scaled by the energy input. Classic theory for inverse cascade spectra gives $U^2 \sim \int \epsilon(k)dk \sim \epsilon^{2/3}k^{-2/3}$ so $U \sim \epsilon^{1/3}k^{-1/3}$

The timescale where non linear terms are balanced by drag is defined when : $\frac{1}{Uk} \sim \frac{1}{r}$
Combining, the two equations above, we find $U \sim \sqrt{\epsilon/r}$ .
Eventually, the wavenumber corresponding to energy dissipation writes :

$$k_H^E = \sqrt{r^3/\epsilon} \tag{2}$$

Hyperviscosity is used in the simulation as a parameter to maximize the enstrophy dissipation in the relatively low wavenumbers. The "classic" viscosity $\nu\nabla^2\omega$ is replaced by the hyper viscosity coefficient $\nu_{hyper}\nabla^n\omega$ This power makes the dissipation far more efficient as we reach higher wavenumber. As for the energy dissipation, we write the scale dissipation of enstrophy wavenumber : $k_H^Z$ The dissipation of enstrophy scale is found after balancing the viscous with the non-linear term :

$$k_H^Z \sim (\frac{\eta^{1/3}}{\nu})^{1/n} \tag{3}$$

The expression is found by balancing the time scales of viscosity and the turnover time of the direct enstrophy cascade. Assuming there is a constant enstrophy flux, we set $\eta = k_f^2\epsilon$

The resolution of the simulations needs to be high enough to dissipate the enstrophy at the scale computed above. We fix the resolution to be at least twice as big as the enstrophy dissipation wavenumber.

### 2.3 Beta-effect

There is a transition between flow dominated by advection at small scale and by the $\beta$-effect at large scales. The balance between the beta term and turbulence is called the Rhines wavenumber, $k_{\beta r}$ and is defined by equating advecting terms and the $\beta$ term.

$$k_{\beta r} = (\frac{\beta}{U})^{1/2} \tag{4}$$

Theoretically, U is the root-mean square velocity at the energy containing scale. It's often mentioned that the Rhines scale is linked with the space between the jets.

Besides, there a scale where linear Rossby waves start to dominate the dynamic of the flow. By equating the eddy turnover time to the Rossby wave period $T_R = \frac{1}{\omega_\beta} \sim \frac{k}{\beta}$. This characteristic wavenumber writes :

$$k_\epsilon = (\frac{\beta^3}{\epsilon})^{1/5} \tag{5}$$

This scale is not necessary the Rhines scale, it's just the scale at which the linear and nonlinear terms reach the same order and so, when Rossby wave motions start to be excited by the background small- scale turbulence.

### 2.4 Introducing Zonostrophy

In order to distinguish the different jet regimes we can use an adimensionnal number, $Z = \frac{k_\epsilon}{k_{\beta r}}$. This number is called Zonostrophy. The approximation of the Rhines scale is computed by using the energy balance $\epsilon = 2r\bar{E}$. We set $U^2 \sim \sqrt{\frac{\epsilon}{r}}$
Considering this,

$$k_{\beta r} = \frac{\beta^{1/2}}{(\frac{\epsilon}{r})^{1/4}} \tag{6}$$

Eventually, the Zonostrophy writes :

$$Z = (\frac{\beta^2\epsilon}{r^5})^{1/20} \tag{7}$$

Which can be seen as the distance between the Rhines scale and the scale where the beta plane begins to be felt.

### 2.5 Introducing Occupation

In a closed domain, the boundaries affect the circulation. It is thus important to consider the size of the domain and its impact on the circulation.

In order to complete the parameter space, we introduce another adimensional parameter which is the ratio between the Rhines length scale and the length of the domain. $Oc = \frac{L_r}{Lx}$

$$Oc \sim \frac{(\frac{\epsilon}{r})^{1/4}}{\beta^{1/2} Lx} \tag{8}$$

"Occupation" characterizes the importance of the a single jet relative to the domain length. A higher Occupation means that a single jet will occupy a larger part of the domain.

## 3 Simulation and Result

### 3.1 Experiment Set up

The experiments start with stochastic forcing at a specific wavenumber $k_f$. To find the values of our parameters and initiate the simulations, we select the Zonostrophy (for the periodic domain, this is the only parameter controlling the jet regime) and the Occupation parameter in addition for the closed domain.

The Zonostrophy sets the drag coefficient, Occupation determines the lengh of the Domain and the enstrophy dissipation scale $k_H^Z$ sets the viscosity. All dimensional parameters we used for all simulations are given in the tables in the appendix A.

The code used for the simulation has been developed by Bruno Deremble and Lennard Miller. This is a QG model using finite difference that rely on FFTW for the elliptic solver. It will be used only with one layer for all simulations.

### 3.2 Results for a Periodic Domain

In the case of a periodic domain, the only adimensional parameter we need is the Zonostrophy. It is varied from 0.67 to 10 while making sure that at least 90% is dissipated by linear drag.

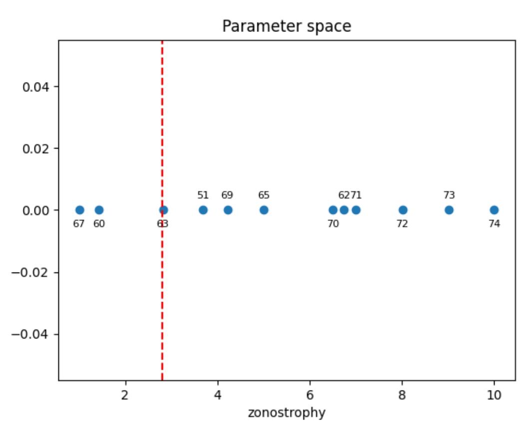


Figure 1: Periodic simulation Zonostrophy value (numbers close to points denote different simulations)

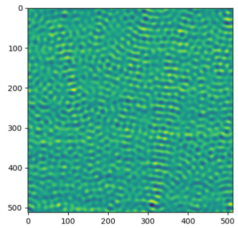

(a) $\psi$ mean for $Z = 1.4$

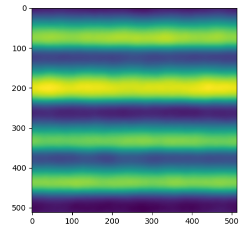

(b) $\psi$ mean for $Z = 3.3$

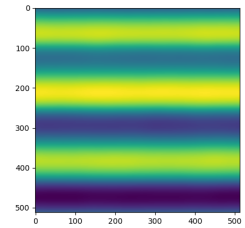

(c) $\psi$ mean for $Z = 10$

Figure 2: Mean streamfunction of the flow for different Zonostrophy in a Periodic domain

The first conclusion is that :

- Below $Z = 2$ there is no turbulence
- Above $\sim Z = 2.6$ we start observing jets (Zonostrophic regime)

When increasing the Zonostrophy, the jets become more distinct, appearing more consistent with less turbulent flow.

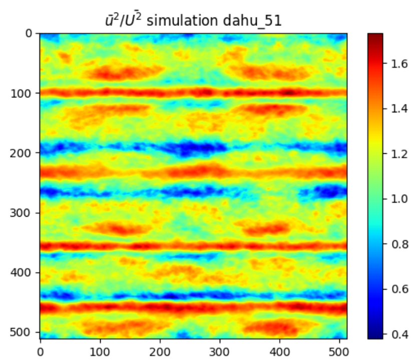


(a) Z=3.3

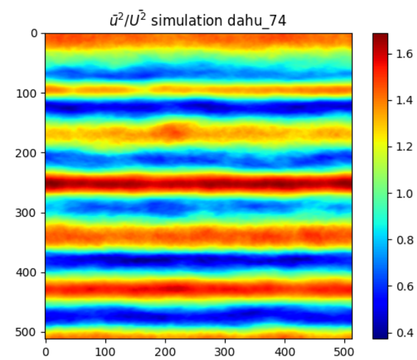


(b) Z=10

Figure 3: Values of $\frac{\bar{u}^2}{\bar{U^2}}$for an increasing increasing Zonostrophy

The Figure 3 illustrates the ratio of kinetic energy contained in the zonal flow to the total mean kinetic energy. For a higher zonostrophy, a greater proportion of energy is distributed within the jets, resulting in a more zonal flow with reduced turbulence.

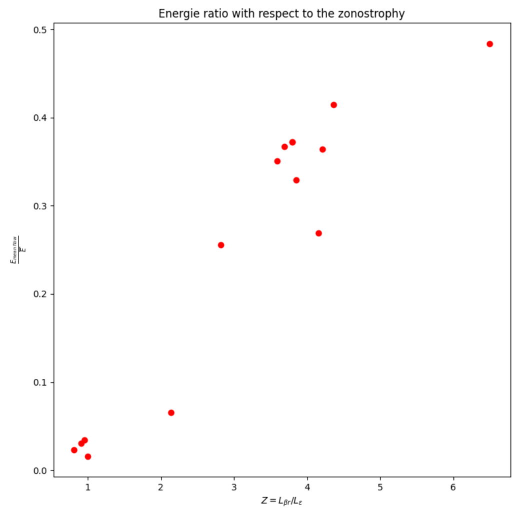


Figure 4: Ratio of the energy in the mean flow over the mean kinetic energy in function of Zonostrophy

The figure 4 shows the ratio between the kinetic energy of the mean flow over the mean kinetic energy $\frac{\overline{u}^2+\overline{v}^2}{u^2+v^2}$ The energy contained in the mean flow increases almost linearly with the Zonostrophy. The turbulence becomes less dominant with higher values of Z.

### 3.3 Results in a closed domain

We now turn to our rectangle periodic domain into a closed domain, imposing free slip boundary conditions. Two adimensional parameters control the different regime : Zonostrophy and the "Occupation" (Figure 4 shows the different simulations we ran in the parameter space). Firstly, what stands out are the two prominent jets at the northern and southern boundaries, which we will refer to as the border jets. To compare with the periodic domain, we initially opt for a weak Occupation to minimize the effect of the length over the jets. However, even with this approach, the jets haven't clearly been observed inside. They should be present, requiring long time averaging of the flow. The figure 4 shows the different simulations run in the parameter space.

When increasing Occupation, the border jets get wider untill reaching the whole size of the domain. For $Oc \geq 1$ a single cell starts to occupy the domain. Nonetheless, in this region, the energy dissipation requirements weren't fulfilled so further runs have to be done.

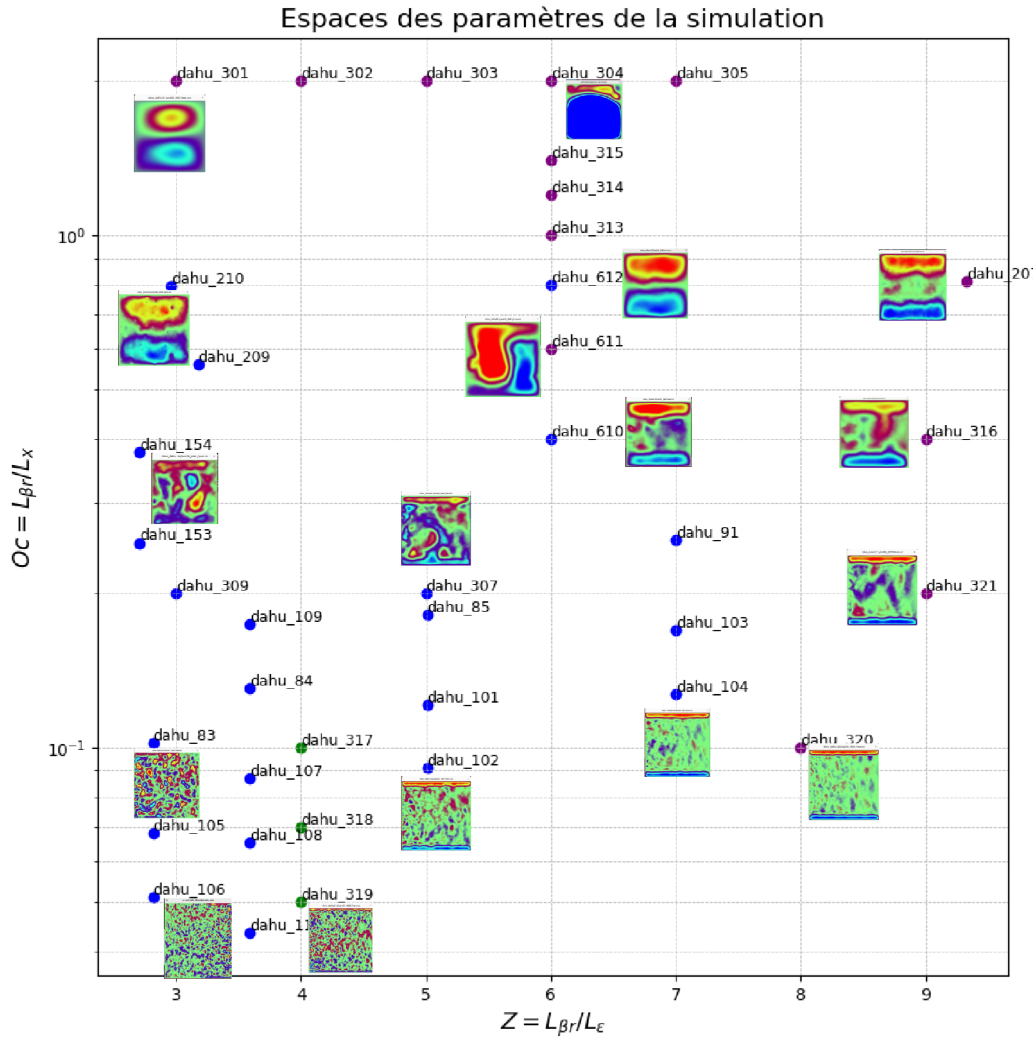


Figure 5: Simulations in the parameters (the plots represent snapshots of the streamfunction)

The blue and green points represent simulations which reach statistical stationarity, while purple simulations don't meet this energy balance requirement. When increasing Zonostrophy, the simulations require longer time of calculation, due to the increase of resolution. This first runs were designed to find the regions with interesting regimes, and better understand what the parameters control. Moreover, for an occupation exceeding 1, the energy evolution wasn't coherent at all, maybe due to the parameters selected, or the running time. We thus won't make further analysis of this area in this report.

Looking at different snapshots, we can identify several regimes. There are regimes with low Occupation and low Zonostrophy where turbulence occupies most part of the domain, zonal jets remain very weak. The regimes with higher Occupation where border jet increase there size. We notice also a similitude with a Fofonoff circulation pattern for an Occupation equal to 0.8.

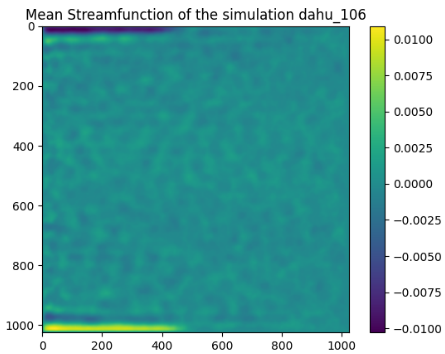


(a) $Oc = 0.05$ $Z = 2.8$

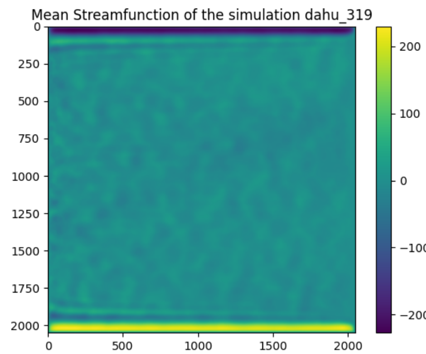


(b) $Oc = 0.05$ $Z = 4$

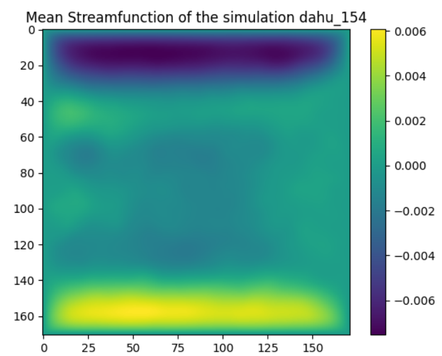


(c) $Oc = 0.4$ $Z = 2.7$

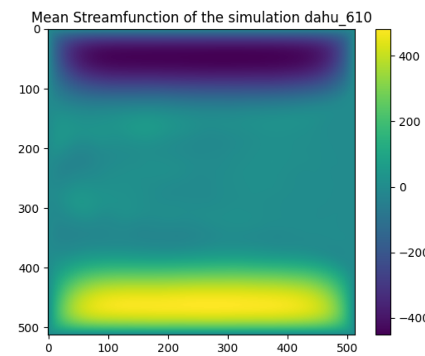


(d) $Oc = 0.4$ $Z = 6$

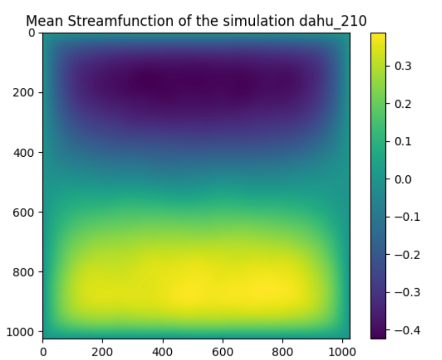


(e) $Oc = 0.8$ $Z = 2.9$

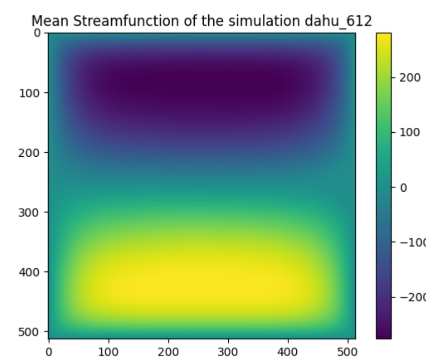


(f) $Oc = 0.8$ $Z = 6$

Figure 6: Values of $\psi$ mean for an increasing Occupation downwards and increasing Zonostrophy rightwards

Like in a periodic domain, the Zonostrophy tend to make the jets more consistent as it increases, with longer filament of vorticity. The figure 6 shows the ratio of the energy contained in the zonal mean flows over the total kinetic energy.

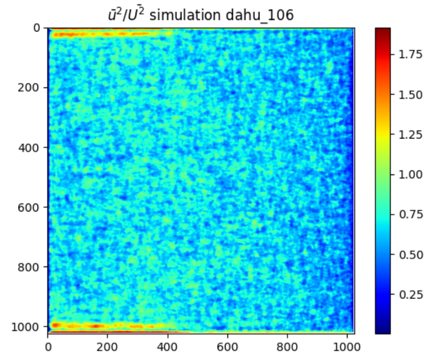


(a) $Oc = 0.05$ $Z = 2.8$

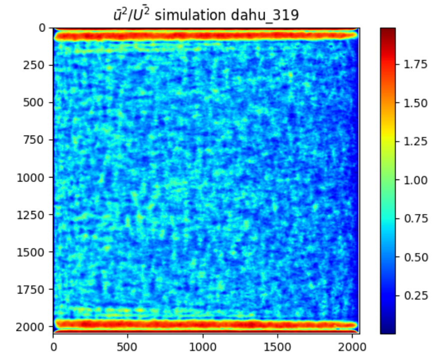


(b) $Oc = 0.05$ $Z = 4$

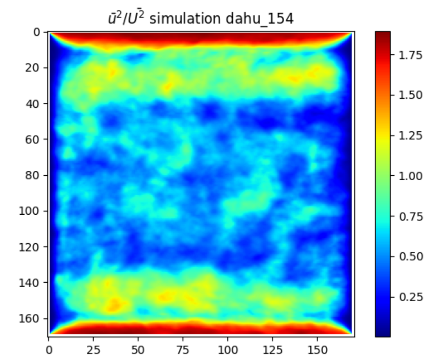


(c) $Oc = 0.4$ $Z = 2.7$

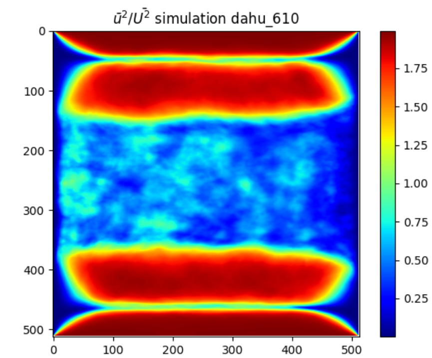


(d) $Oc = 0.4$ $Z = 6$

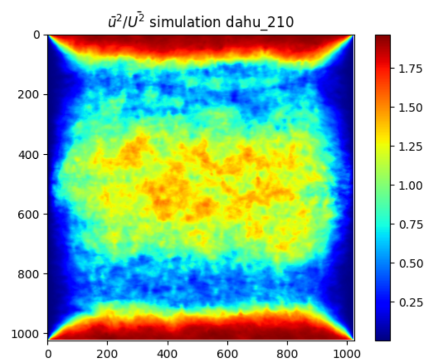


(e) $Oc = 0.8$ $Z = 2.9$

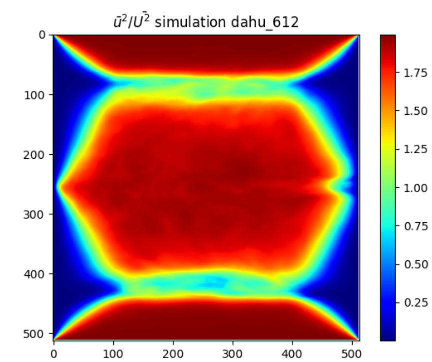


(f) $Oc = 0.8$ $Z = 6$

Figure 7: Values of $\frac{\bar{u}^2}{\bar{U^2}}$ for an increasing Occupation downwards and increasing Zonostrophy rightwards

The zonal kinetic energy is mainly concentrated at the top borders of the domain, in the areas of circulation corresponding to the border jets.

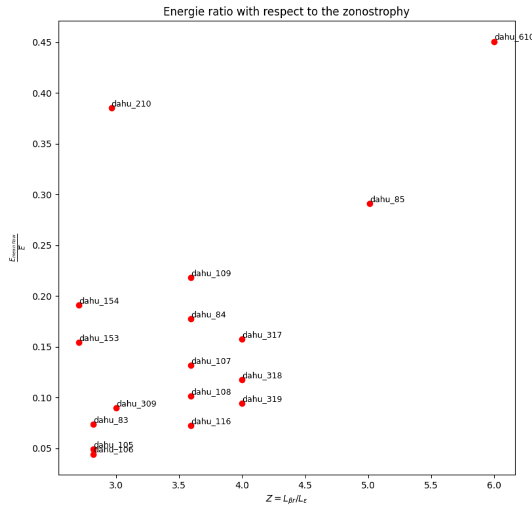


Figure 8: Ratio of the energy in the mean flow over the mean kinetic energy in function of Zonostrophy

In this case, Energy in the jets also appears to depend on the Occupation as can be seen by the larger spread in the data 8.

# 4 Conclusion

In conclusion, the simulations in a closed domain show interesting characteristics. Their most noticeable point is the two significant border jets. Their size depend on the ratio between the Rhines scale and the size of the domain we called the "Occupation". This parameter also influences the energy in the mean flow.

# A Appendix A

| Simu No | f0 | beta | r | Lx | nx | ny | sigma_f | bc_fac | nu_hyper | n_hyper |
|---|---|---|---|---|---|---|---|---|---|---|
| 59 | 2.0 | 4.0 | 7.000e-03 | 6.283e+00 | 512.0 | 512.0 | 2.000e-03 | -1.0 | 9.000e-15 | 6.0 |
| 47 | 2.0 | 2.0 | 5.000e-04 | 6.283e+00 | 512.0 | 512.0 | 2.000e-03 | -1.0 | 9.000e-15 | 6.0 |
| 48 | 2.0 | 7.0 | 5.000e-04 | 6.283e+00 | 512.0 | 512.0 | 2.000e-03 | -1.0 | 9.000e-15 | 6.0 |
| 49 | 2.0 | 3.0 | 3.000e-01 | 6.283e+00 | 512.0 | 512.0 | 2.000e-03 | -1.0 | 9.000e-15 | 6.0 |
| 51 | 2.0 | 3.0 | 7.000e-04 | 6.283e+00 | 512.0 | 512.0 | 2.000e-03 | -1.0 | 9.000e-15 | 6.0 |
| 52 | 2.0 | 1.5 | 1.200e-01 | 6.283e+00 | 512.0 | 512.0 | 2.000e-03 | -1.0 | 9.000e-15 | 6.0 |
| 53 | 2.0 | 10.0 | 7.000e-04 | 6.283e+00 | 512.0 | 512.0 | 2.000e-03 | -1.0 | 9.000e-15 | 6.0 |
| 54 | 2.0 | 9.0 | 3.000e-01 | 6.283e+00 | 512.0 | 512.0 | 2.000e-03 | -1.0 | 9.000e-15 | 6.0 |
| 63 | 2.0 | 4.0 | 2.300e-03 | 6.283e+00 | 512.0 | 512.0 | 2.000e-03 | -1.0 | 9.000e-15 | 6.0 |
| 64 | 2.0 | 4.0 | 8.700e-04 | 6.283e+00 | 512.0 | 512.0 | 2.000e-03 | -1.0 | 9.000e-15 | 6.0 |
| 68 | 2.0 | 4.0 | 6.950e-04 | 6.283e+00 | 512.0 | 512.0 | 2.000e-03 | -1.0 | 9.000e-15 | 6.0 |
| 67 | 2.0 | 4.0 | 1.450e-01 | 6.283e+00 | 512.0 | 512.0 | 2.000e-03 | -1.0 | 9.000e-15 | 6.0 |
| 70 | 2.0 | 4.0 | 8.120e-05 | 6.283e+00 | 512.0 | 512.0 | 2.000e-03 | -1.0 | 9.000e-15 | 6.0 |
| 69 | 2.0 | 4.0 | 4.600e-04 | 6.283e+00 | 512.0 | 512.0 | 2.000e-03 | -1.0 | 9.000e-15 | 6.0 |
| 68 | 2.0 | 4.0 | 6.950e-04 | 6.283e+00 | 512.0 | 512.0 | 2.000e-03 | -1.0 | 9.000e-15 | 6.0 |

Figure 9: Table of parameter values for the periodic domain

| Simu No | f0 | beta | r | Lx | nx | ny | sigma_f | bc_fac | nu_hyper | n_hyper |
|---|---|---|---|---|---|---|---|---|---|---|
| 83 | 2.0 | 4.0 | 2.300e-03 | 6.283e+00 | 512.0 | 512.0 | 2.000e-03 | 0.0 | 9.000e-15 | 6.0 |
| 84 | 2.0 | 4.0 | 8.700e-04 | 6.283e+00 | 512.0 | 512.0 | 2.000e-03 | 0.0 | 9.000e-15 | 6.0 |
| 85 | 2.0 | 4.0 | 2.300e-04 | 6.283e+00 | 512.0 | 512.0 | 2.000e-03 | 0.0 | 9.000e-15 | 6.0 |
| 116 | 2.0 | 4.0 | 8.700e-04 | 1.885e+01 | 2048.0 | 2048.0 | 2.000e-03 | 0.0 | 9.000e-15 | 6.0 |
| 153 | 2.0 | 2.66 | 2.300e-03 | 3.142e+00 | 300.0 | 300.0 | 2.000e-03 | 0.0 | 9.000e-15 | 6.0 |
| 154 | 2.0 | 2.66 | 2.300e-03 | 2.094e+00 | 170.0 | 170.0 | 2.000e-03 | 0.0 | 9.000e-15 | 6.0 |
| 210 | 2.0 | 0.66 | 2.300e-03 | 6.283e+00 | 1024.0 | 1024.0 | 2.000e-02 | 0.0 | 9.000e-15 | 6.0 |
| 309 | 2.0 | 1.0 | 1.235e-02 | 9.425e+01 | 512.0 | 512.0 | 1.000e+00 | 0.0 | 3.906e-03 | 4.0 |
| 610 | 2.0 | 1.0 | 7.716e-04 | 9.425e+01 | 512.0 | 512.0 | 1.000e+00 | 0.0 | 7.716e-04 | 4.0 |
| 317 | 2.0 | 1.0 | 3.906e-03 | 2.513e+02 | 1024.0 | 1024.0 | 1.000e+00 | 0.0 | 7.716e-04 | 4.0 |
| 318 | 2.0 | 1.0 | 3.906e-03 | 3.590e+02 | 2048.0 | 2048.0 | 1.000e+00 | 0.0 | 7.716e-04 | 4.0 |
| 319 | 2.0 | 1.0 | 3.906e-03 | 5.027e+02 | 2048.0 | 2048.0 | 1.000e+00 | 0.0 | 7.716e-04 | 4.0 |
| 105 | 2.0 | 4.0 | 2.300e-03 | 9.425e+00 | 768.0 | 768.0 | 2.000e-03 | 0.0 | 9.000e-15 | 6.0 |
| 106 | 2.0 | 4.0 | 2.300e-03 | 1.257e+01 | 1024.0 | 1024.0 | 2.000e-03 | 0.0 | 9.000e-15 | 6.0 |
| 107 | 2.0 | 4.0 | 8.700e-04 | 9.425e+00 | 768.0 | 768.0 | 2.000e-03 | 0.0 | 9.000e-15 | 6.0 |
| 108 | 2.0 | 4.0 | 8.700e-04 | 1.257e+01 | 1024.0 | 1024.0 | 2.000e-03 | 0.0 | 9.000e-15 | 6.0 |
| 109 | 2.0 | 4.0 | 8.700e-04 | 4.712e+00 | 384.0 | 384.0 | 2.000e-03 | 0.0 | 9.000e-15 | 6.0 |

Figure 10: Table of parameter values for the non periodic domain